frontiers in Energy Research

BRIEF RESEARCH REPORT
published: 22 June 2021
doi: 10.3389/fenrg.2021.682709

Application of Bunchy TiO_2 Hierarchical Microspheres as a Scattering Layer for Dye-Sensitized Solar Cells

Yongjian Jiang[1] *and Fengyang Zhao*[2]*

[1]College of Science, Liaoning Petrochemical University, Fushun, China, [2]College of Chemistry and Material Science, Liaoning Petrochemical University, Fushun, China

A novel bunchy TiO_2 hierarchical microspheres composite nanostructure with strings of anatase TiO_2 hierarchical micro-spheres and rutile nanobelts framework (HSN) was synthesized via an one-pot hydrothermal process. This new structure presents great specific surface area, large pore size distribution, homogeneous three-dimensional (3D) structure, high crystallinity and excellent light scattering performance simultaneously. The bi-layer photoanode film was successfully prepared which TiO_2 P25 as absorption layer and HSN as an efficient scattering layer on the top of TiO_2 P25 film in dye sensitized solar cells (DSSC). The bi-layer DSSC taken on a great progress in the power conversion efficiency (PCE) achieved 8.08%. However, the PCE of single and double layer TiO_2 film DSSCs just showed 6.72% and 3.67% respectively. Such improvement was mainly because of the efficient scattering centers (HSN) which can bring the enhanced dye loading, fast charge transfer and excellent light harvesting efficiency.

Keywords: dye sensitized solar cells, bunchy TiO2 hierarchical microspheres (HSN), bi-layer DSSCs, scattering layer, charge transfer

OPEN ACCESS

Edited by:
Su Pei Lim,
Xiamen University, Malaysia

Reviewed by:
Dillip K. Panda,
Clemson University, United States
Shanmuga Priya S,
Manipal Institute of Technology, India

Correspondence:
Fengyang Zhao
a406280751@163.com

Specialty section:
This article was submitted to Solar Energy, a section of the journal Frontiers in Energy Research

Received: *19 March 2021*
Accepted: *20 May 2021*
Published: *22 June 2021*

Citation:
Jiang Y and Zhao F (2021) Application of Bunchy TiO_2 Hierarchical Microspheres as a Scattering Layer for Dye-Sensitized Solar Cells. Front. Energy Res. 9:682709. doi: 10.3389/fenrg.2021.682709

INTRODUCTION

The central energy source elated from the extraterrestrial space, solar energy capacities to surpass the almanac world's energy request by a large border. Given the long forecast era of the sun, solar energy is also considered the ultimate renewable source that can be harvested on the planet, earth. In 1991, a new photoelectric converter which named dye-sensitized solar cell (DSSC) was successfully prepared under appropriate process conditions by O'Regan and Gratzel (Oregan and Grätzel, 1991). Thereafter, DSSC has gained wide attention recent years as potential low-cost solar cells, owing to their simple manufacturing process, environmentally friendly material and relatively high power conversion efficiency (PCE) (Chen et al., 2017; Ponken et al., 2019; Ünlü and Özacar, 2020). Until now, a η of nearly 14% has been presented. Normally, photoanode material, the key component of the DSSC, plays a decisive role for preparing highly efficient DSSCs (Lee et al., 2014; Park and Dhayal, 2014; Jang et al., 2015; Wang et al., 2015). For example, the thin TiO_2 photoelectrode can absorb dye sensitizer, transfer photo generated electrons to the conductive substrate fluorine-doped tin oxide (FTO) and promote the diffusion of electrolyte into the adsorbed dye (Steffy et al., 2017; Maurya et al., 2019). Among the semiconductor metal-oxides, nanostructures TiO_2 materials have been widely utilized as an efficient mediator to transfer electrons and promote the separation of photoinduced electron-hole pairs in the working electrode of the DSSCs (Jadhav et al., 2014; Chandrakala et al., 2016). In the past few years, a lot of studies had been concentrated on design and preparation of excellent TiO_2 photoanode materials. It is well-known that two requirements are desirable for satisfactory photoanode materials, one is the large specific surface area for more dye loading and the other is the uniform structure for more optical scattering and faster electronic transmissions (Hore et al., 2006; Zhang et al., 2019). So it is highly desirable if one could simply prepare unique TiO_2 nanostructures with a large specific surface area which will promote their widely used in DSSCs.

Herein, we successfully synthesized TiO_2 HSN via one-step hydrothermal method by using TiO_2 nanobelts as growing framework, tetrabutyl titanate (TBOT) as titanium source, and the glacial acetic acid (HAC) solutions as regulating agent. This novel micro-sized material and TiO_2 P25 were used to fabricated the bi-layer TiO_2 photoanode film based DSSC, in which the photoanode consisting of the nano-sized TiO_2 P25 film as under-layer and the micro-sized TiO_2 HSN film as upper-layer. This is a larger breakthrough in preparing a double layered TiO_2 photoanode DSSC.

EXPERIMENTAL

Synthesis of HSN and Preparation of Dye-Sensitized Solar Cell

The preparation of HSN had been described in detail in our previous work (Jiang et al., 2014). In brief, the prepared nanobelts (Wang et al., 2008) were firstly taken into a mixed solutions of 160 ml HAC, 2.0 ml TBOT and 0.4 g $AgNO_3$. Next the mixed solution was stirred constantly until just combined, and then poured into the high pressure reactor (100 ml), and conducted in drying oven for 6 h at 150°C. After the reaction process, the obtained products were washed by absolute alcohol and deionized water for many times until neutral, then calcined in box type heater for 30 min at 450°C. The configuration process of photoanode slurry and assembly process of dye-sensitized cell were introduced in detail in our previous work (Jiang et al., 2013). The only difference is that the photoanode film changes from single layer to multi-layer. For details: firstly, a paste of TiO_2 P25 was deposited onto the FTO substrate, dried at room temperature, then calcined for 35 minutes at 450°C. After that, the prepared TiO_2 HSN slurry was spread on the P25 film electrode, and then calcined at 450°C for 35 minutes.

Sample Characterization

The crystal structure of TiO_2 HSN was studied by X-ray powder diffraction (XRD), and the XRD measurement is presented in our previous work (Jiang et al., 2014). The morphology of HSN was observed by FEI SIRION 200) Scanning Electron Microscopy (SEM) and high-resolution transmission electron microscopy (TEM/HRTEM) operated by JEM-200CX, equipped with selected area electron diffraction (SAED) of the sample. The specific surface area of HSN and TiO_2 P25 were both measured by the Brunauer-Emmet-Teller (BET) with a N_2 adsorption tester (Micromeritics ASAP 2020). Diffuse reflection spectra of single TiO_2 P25 electrode and TiO_2 bi-layer electrode were both measured using a UV-vis spectrophotometer (UV 2600 Shimadzu). The dye loading capacity of different photoanodes (P25, P25/P25, P25/HSN) were measured by the same method in our previous work (Zhao et al., 2018). Photovoltaic properties, electrochemical impedance spectroscopy (EIS) and incident-photon-to-current efficiency (IPCE) spectra of the cells were measured with the same method as described in the previous work (Jiang et al., 2013).

RESULTS AND DISCUSSION

TiO_2 HSN was prepared using the hydrothermal synthesis method, the main factors influencing HSN growth process were investigated in our previous work (Jiang et al., 2014). The morphology of the prepared HSN is shown in **Figure 1**. As we can see, high homogeneous bunchy structures composed of plentiful micro-spheres, and the regular array of 3D TiO_2 micro-spheres are consist of a large number of TiO_2 thin nanosheets. Furthermore, we can see clearly from **Figures 1A,B**, the diameter of self-assembly micro-spheres are nearly 1.5 μm, meanwhile, a nanobelt with a dozen microns length acts as the growing framework **Figure 1C** which throughout the structure (**Figures 1B,C**). More interestingly, a large number of TiO_2 nanoparticles adhere to the 2D TiO_2 nanosheets, and the measurement shows that the diameter of every nanoparticle is about 10–30 nm, as shown in **Figure 1D**. We all know that the existence of tiny nanoparticles will greatly increase the specific surface area of new structural materials.

For detailed analysis, the edge of the micro-spheres image is also shown in **Figure 1**. We can see the nanosheets and nanoparticles clearly in **Figure 1D**, the local regions landmarks are corresponds to the **Figures 1E,F**. As stated earlier, the internal section exhibits better crystallized state, and there are clear lattice fringes on the nanosheets and nanoparticles. As show in **Figure 1E**, the lattice spacing of ~0.235 nm and ~0.35 nm are calculated at the edge of nanosheet which coincide with the (001) and (101) crystal planes belong to anatase TiO_2. While **Figure 1F** shows the lattice distance to the nanoparticals facets is *ca* 0.19 nm, which coincides well with (110) crystal planes of anatase TiO_2. It has been proved by many researches that anatase TiO_2 especially high exposure (001) crystal planes has great advantages in the field of DSSCs (Khalil et al., 2019; Lara et al., 2019; Wang et al., 2019).

The adsorption property of TiO_2 HSN and TiO_2 P25 were further determined. **Figure 2A** and **Figure 2B** show N_2 adsorption isotherms and pore size distribution curves of TiO_2 P25 and TiO_2 HSN. The related parameters are summarized in **Table 1**. By the full analysis of the curve in **Figure. 2A**, TiO_2 HSN exhibits a loose and mesoporous structure, which displays a typical type IV isotherms on the basis of IUPAC classification, and the S_{BET} of the TiO_2 HSN and TiO_2 P25 are 144.432 m^2/g and 50.025 m^2/g, respectively. Obviously, the novel product shows relatively higher specific surface areas, which is beneficial to the adsorption of dyes for DSSC. Furthermore, the average pore volume and average pore diameters of the TiO_2 HSN are 1.048 cm^3/g and 61.463 nm , for P25 are only 0.6693cm^3/ g and 18.805 nm. Prior studies have suggested that the advantageous large pore size distributions is beneficial to facilitate the fast diffusion of ions in electrolyte (Zhao et al., 2018).

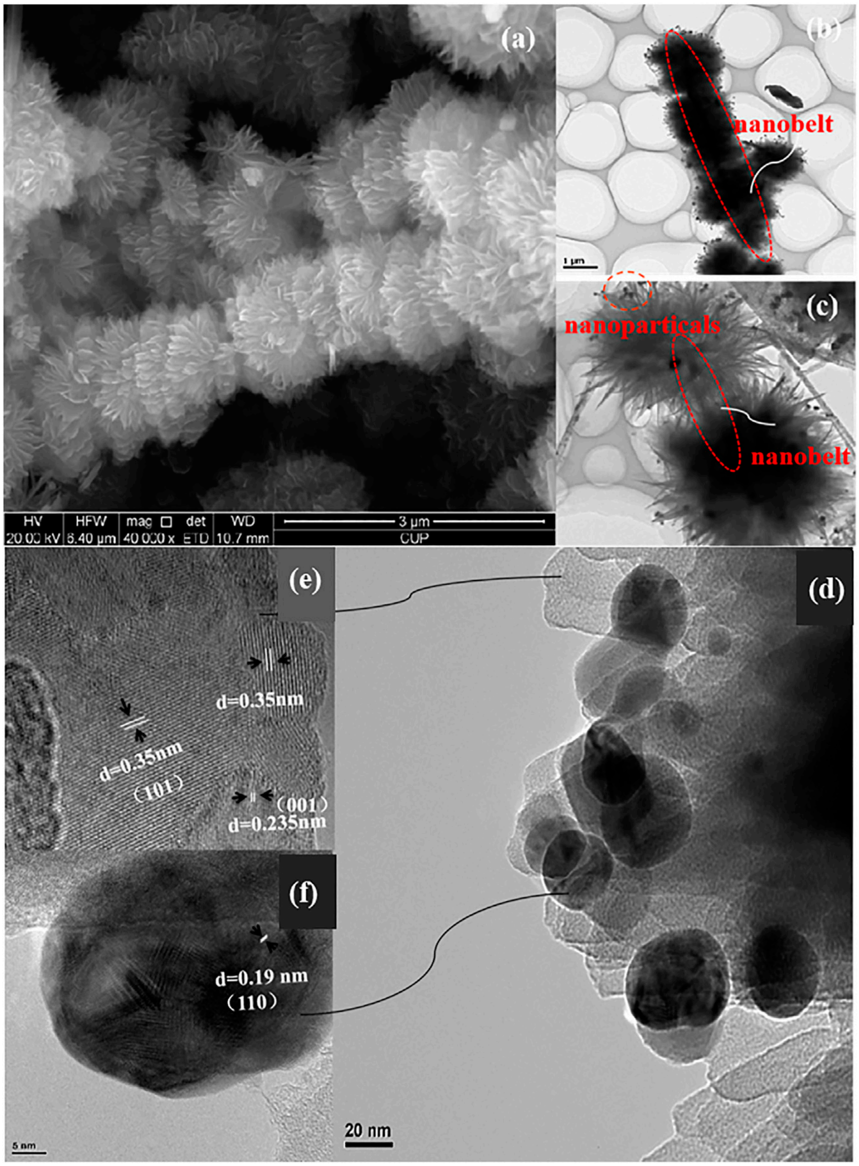

FIGURE 1 | Magnification **(A)** SEM, TEM **(B)** and HRTEM **(C)** of the prepared HSN; HRTEM of the prepared HSN; **(D)**: the lattice spacing parallel of thenanosheet **(E)** and the nanoparticals **(F)** in HSN.

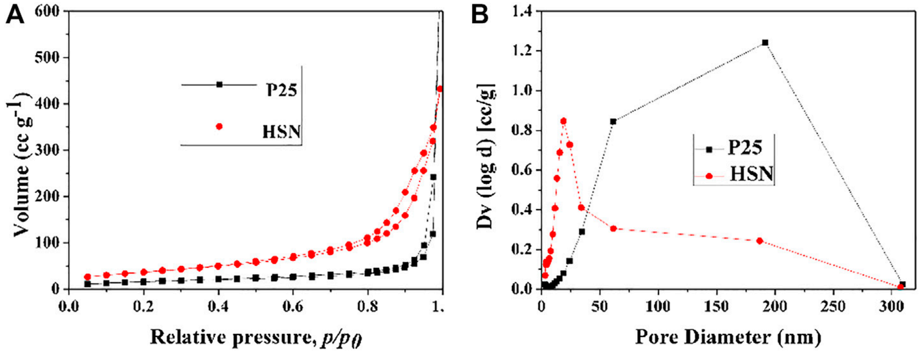

FIGURE 2 | N_2 adsorption isotherms **(A)** and pore size distribution curves **(B)** of TiO_2 HSN and P25.

TABLE 1 | Physical parameters of TiO_2 HSN and P25 films with N_2 adsorption tester.

Samples	SBET (m2/g)	Pore volume (cm^3/g)	Average pore diameter (nm)
P25	50.025	0.6693	18.805
HSN	144.432	1.048	61.463

As we know, photoanode films made from pure nano-sized TiO_2 particles usually exhibit low light harvesting efficiency. Therefore, the photoanode films with the scattering layer are very essential which can effectively increase the propagation path of sunlight (Chava et al., 2017; Cui et al., 2017; Xu et al., 2019; Xie et al., 2020). N_2 adsorption experiments show that the novel TiO_2 HSN with huge specific surface area and the uniform nanosheets structure is an excellent scattering layer for DSSC. In our study, in order to verify the effect of HSN scattering layer, three different photoanode films (P25 13 μm, P25 13 μm /P25 7 μm, P25 13 μm /HSN 7 μm) were prepared. The cross-sectional images of the pure P25 electrode (P25), P25 absorbent layer/ P25 scattering layer (P25/P25) and P25/HSN scattering layer (P25/HSN) are shown in **Figure.3**. It can be seen from **Figures 3A,B**, the individual TiO_2 P25 films are 13 μm and 20 μm thick (can be considered to 13 μm absorbing layer and 7 μm scattering layer) respectively. Meanwhile, the bi-functional structure layer of P25/HSN which consist of 13 μm P25 absorbing layer and 7 μm HSN scattering layer is shown in **Figure 3C**. Even better, for ease of understanding, the schematic diagram of the P25/HSN photoanode DSSC device is vividly depicted, as shown in **Figure 3D**.

In order to validate the light scattering effect, the reflectance spectra of P25 (13 μm) photoanode film, TiO2 P25 (20 μm) photoanode film and P25/HSN photoanode film were investigated. As shown in **Figure 4A**, the P25/HSN photoanode with HSN scattering layer exhibits the strongest reflectivity which is ascribed to the potential scattering properties of the unique HSN structure. Several studies have described that the scattering materials with a size similar to the wavelength of visible light could cause great light dispersion effect on the basis of Mie theory (Konevskikh et al., 2018). Accordingly, the upper-layer TiO_2 HSN can reflect most of sunlight to the under-layer TiO_2 P25, which can improve the utilization of sunlight. Further, after dye adsorption process, the UV-vis absorption spectras of the three photoanode films were tested, as shown in **Figure 4B**, the P25/HSN photoanode film shows the best light absorption property on the full spectrum. It is verified that the addition of TiO_2 HSN will greatly improve the efficient utilization of sunlight.

The current-voltage (I-V) characteristics of the three cells were tested, the results are shown in **Figure 4C**, and the main performance parameters are summarized in **Table 2**. The cell P25 (13 μm) exhibits a short-circuit current (Jsc) of 13.64 mA/cm2 and PCE of 6.72%, whereas cell P25 (20 μm) only attains a 11.44 mA/cm2 and PCE of 3.67%, and there is 45.39% decrease in PCE compared to cell P25 (13 μm). Conspicuously, cell with HSN as the scattering layer (cell P25/HSN) demonstrates the highest Jsc (17.86 mA/cm^2) among the three cells, while the voltage and fill factor (FF) remain similar with P25 (13 μm) cells. As a result, the PCE increases to the hightest of 8.08%, corresponding to

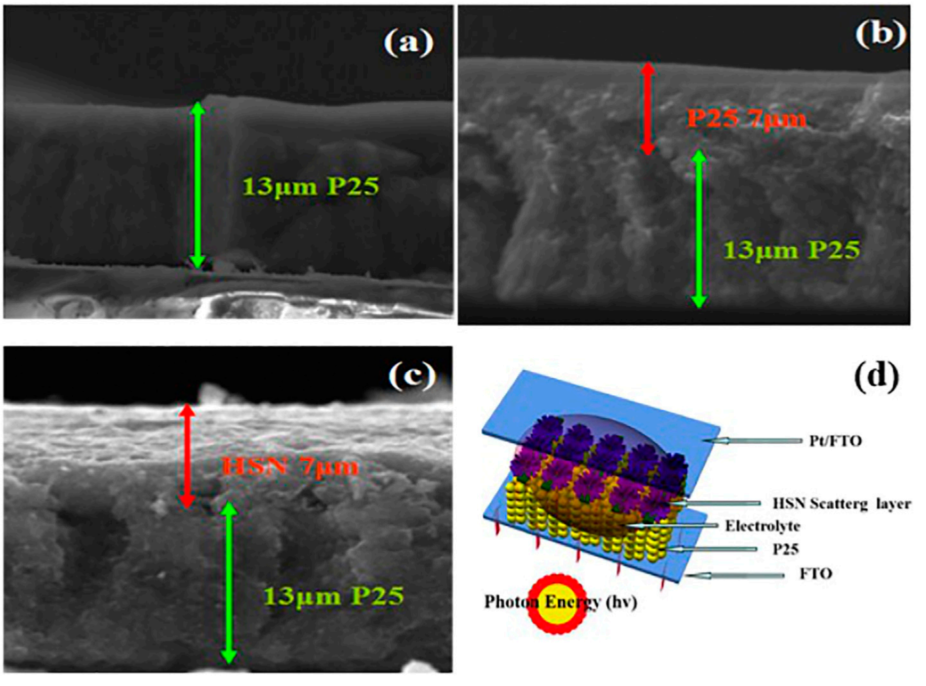

FIGURE 3 | SEM of cross-section of the individual photoanodes : **(A)** single layer photoanode of TiO_2 P25 (13 μm), **(B)** bi-layer film consists of TiO_2 P25 absorbing layer (13 μm) and TiO_2 P25 scattering layer (7 μm), **(C)** bi-layer film consists of TiO_2 P25 absorbing layer (13 μm) and TiO_2 HSN scattering layer (7 μm); **(D)** schematic diagram of the DSSC device, in which the photoanode consists of the TiO_2 P25 film as under-layer and the TiO_2 HSN film as upper-layer.

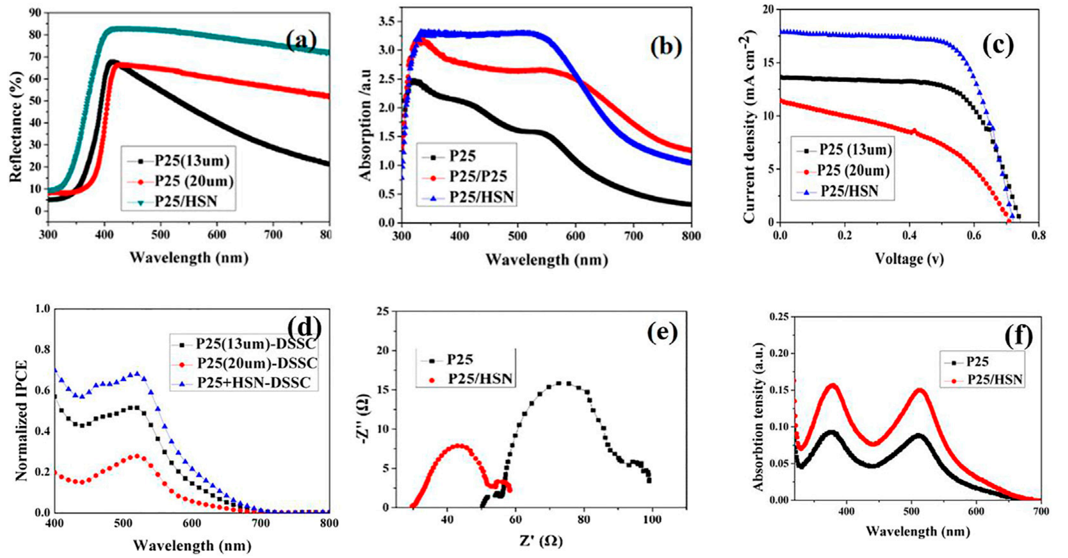

FIGURE 4 | (A) Diffuse reflectance spectra before dye adsorption; **(B)** Absorption spectra after the dye adsorption of the photoanode films; **(C)** Current-voltage (IV) curves **(D)** IPCE spectra of the cells with P25 (13 μm), P25 (20 μm) and P25/HSN electrodes under one sun illumination; **(E)** EIS curves of P25 (13 μm) cell and P25/HSN cell; **(F)** The optical absorption spectra of dye loading in TiO_2 P25 (13 μm), P25/HSN electrodes.

20.24% increment compared to cell P25 (13 μm). However, the cell with P25 (20 μm) photoanode shows the worst power conversion efficiency which attributes to the high recombination of electron-hole pairs of TiO_2 nanoparticals. So further enhancing the thickness of the TiO_2 P25 film can not increase the PCE, even if the adsorption quantity of dye increases. By a detailed analysis, the P25/HSN cell shows the best power conversion efficiency.

In order to compare the effects of different photoanode films (P25/HSN and P25 [13 μm, P25 (20 nm)] on photocurrent of DSSCs, the internal quantum efficiency were measured via IPCE measurement. The result reflects that the morphology, size, porosity and S_{BET} of the photoanode materials all influence the IPCE data (Sauvage et al., 2010; Kavan et al., 2011; Xue et al., 2012). As shown in **Figure 4D**, P25/HSN photoanode cell exhibits the highest IPCE at 530 nm. In addition, because of the large specific surface area of HSN which obviously boost the dye adsorption, the P25/HSN-DSSC shows a better performance on IPCE from 400 nm to 600 nm wavelength. More significantly, due to the participation of HSN, P25/HSN cell also shows excellent values in the wavelength range of 600–700 nm. Based on the analysis of the basic characteristics (has low absorption ability in the region of 600–700 nm of N719), the excellent scattering performance of TiO_2 HSN leads to the high optical energy utilization ratio in the wavelength range of 600–700 nm. Stated thus, the enhanced photocurrent of P25/HSN-DSSC is mainly attributed to the coordinated actions of excellent dye adsorption and strong scattering performance of TiO_2 HSN. In a follow-up experiment, we studied for only P25 (13 μm)-DSSC and bi-layer P25/HSN-DSSC.

The electron transport and recombination properties at the photoanode films-dye-electrolyte interface were also tested by using electrochemical impedance spectroscopy (EIS)(Wang et al., 2005). As we can see, two well-defined semicircles are shown in **Figure 4E**, since the impedance of other components unchanged, we only focus on the curves in multi-channel which represents the electron transfer/charge recombination at the photoanode film-dye-electrolyte interface. At last, the values of charge transfer resistance (Rct) have been calculated, for P25 (13 μm) cell is 35 Ω, and for P25/HSN cell is only 21 Ω. Therefore, we can say that the existence of TiO_2 1D namobelts and 2D nanosheets lead to the more excellent redox ability of I^{3-}/I^- pairs at photoanode-dye-electrolyte interface, and thus the lower Rct of P25/HSN-DSSC.

In order to study the dye adsorption properties of different photoanode films, dye adsorption-desorption experiment of photoanode films were studied. **Figure 4F** shows the optical absorption spectra of all photoanode films, and the adsorption quantities of dye by P25 and P25/HSN photoanodes are presented

TABLE 2 | Comparison of relevant parameters for cells Based on Photoanodes of P25 (13 μm), P25 (20 μm) and P25/HSN.

Samples	Thickness (μm)	V_{OC} (V)	J_{SC} (mA cm^{-2})	FF	PCE (%)	Absorbed dye (μmol/cm^2)
P25 (13 μm)	13	0.74	13.64	0.67	6.72	95.1
P25 (20 μm)	20	0.71	11.44	0.45	3.67	130.2
P25/HSN	20	0.72	17.86	0.63	8.08	160.6

in **Table 2**. It indicates that when using the P25/HSN photoanode, dye adsorption capacity is enhanced , thus the absorption of sunlight is increased. To further prove the superiority of TiO_2 HSN as a scattering layer, the dye adsorption amount of the photoanode film with a 20 μm thick P25 layer was also measured by the same method. As shown in **Table 2**, the loading amount of dyes in P25 (20 μm) photoanode is obviously improved when increasing the thickness of the P25 film, nevertheless, the J_{SC}, V_{OC}, FF all decrease compared to the P25 (13 μm), which attributes to the thicker P25 film brings more recombination sites. Therefore, it also shows that the dye loading does not the most important factor affecting the efficiency of DSSCs. The good scattering ability and excellent electronic transmission performance of the HSN are of great significance in improving the performance of DSSCs.

CONCLUSION

In summary, a novel bunchy TiO_2 hierarchical nanostructure was successfully synthesized via facile hydrothermal approach. The TiO_2 hierarchical nanostructure is assembled by anatase nanosheet based microspheres and nanobelt framework. The new TiO_2 structure shows excellent dye adsorption capability and powerful scattering ability. The TiO_2 HSN act as a scattering layer in photoanode film for DSSCs, which can greatly enhance the performance of DSSCs. The PCE of the P25/HSN-DSSC has reached 8.08%, showing a 20.24% increment over that derived from DSSC with single-layer nanocrystalline TiO_2 P25. The experimental results can be explained by the several favorable potential advantages of TiO_2 HSN scattering layer which can offer large specific surface area, excellent light scattering capability and direct electron transport pathways. It is evidential from the findings of this work that the novel TiO_2 HSN could be promising photoanode systems for DSSC applications.

DATA AVAILABILITY STATEMENT

The raw data supporting the conclusion of this article will be made available by the author, without undue reservation.

AUTHOR CONTRIBUTIONS

FZ: Purchase materials and instruments, analyze experimental data, and revise papers YJ: Design the experiment plan, do the experiment, write the paper.

FUNDING

The work was supported by National Natural Science Foundation of China (No. 21808096),Fundamental Research Funds for the Doctors of Liaoning Provincial Natural Science Foundation (No. 20170520259), Scientific Research Fund of Liaoning Provincial Education Department (NO. L2017LQN003, L2017LQN036) and Talent Scientific Research Fund of LSHU (No. 2016XJJ-071, 2016XJJ-088).

REFERENCES

Chandrakala, V., Annai Joseph Steffy, J., Bachan, N., Jothi Jeyarani, W., Tenkyong, T., and Shyla, J. M. (2016). A Comparative Investigation of Dye-Sensitized Titanium Dioxide (TiO2) Nanorods Grown on Indium Tin Oxide (ITO) Substrates by Direct and Seed-Mediated Hydrothermal Methods. *Acta Metall. Sin. (Engl. Lett.* 29, 457–463. doi:10.1007/s40195-016-0409-y

Chava, R. K., Lee, W.-M., Oh, S.-Y., Jeong, K.-U., and Yu, Y.-T. (2017). Improvement in Light Harvesting and Device Performance of Dye Sensitized Solar Cells Using Electrophoretic Deposited Hollow TiO2 NPs Scattering Layer. *Solar Energ. Mater. Solar Cell* 161, 255–262. doi:10.1016/j.solmat.2016.11.037

Chen, C.-N., Wu, M.-J., Hsu, C.-F., and Huang, J.-J. (2017). Antireflection Coating of SiO 2 Thin Film in Dye-Sensitized Solar Cell Prepared by Liquid Phase Deposition. *Surf. Coat. Tech.* 320, 28–33. doi:10.1016/j.surfcoat.2017.02.015

Cui, Y., He, X., Zhu, M., and Li, X. (2017). Preparation of Anatase TiO2 Microspheres with High Exposure (001) Facets as the Light-Scattering Layer for Improving Performance of Dye-Sensitized Solar Cells. *J. Alloys Comp.* 694, 568–573. doi:10.1016/j.jallcom.2016.10.032

Hore, S., Vetter, C., Kern, R., Smit, H., and Hinsch, A. (2006). Influence of Scattering Layers on Efficiency of Dye-Sensitized Solar Cells. *Solar Energ. Mater. Solar Cell* 90, 1176–1188. doi:10.1016/j.solmat.2005.07.002

Jadhav, N. A., Singh, P. K., Rhee, H. W., Pandey, S. P., and hattacharya, B. B. (2014). Effect of Structure Texture and Morphology Modulation on Efficiency of Dye Sensitized Solar Cells. *Electrochem* 9, 5377–5388. doi:10.13140/2.1.1394.4961

Jang, H. D., Jo, E. H., Chang, H., Kim, J., and Roh, K. M. (2015). Incorporation of 3D Crumpled Graphene in Nanostructured TiO2 Films for Dye-Sensitized Solar Cells. *Mater. Lett.* 142, 304–307. doi:10.1016/j.matlet.2014.12.078

Jiang, Y., Li, M., Ding, R., Song, D., Trevor, M., and Chen, Z. (2013). Enhanced the Performance of Dye-Sensitized Solar Cells with a Novel Photoanode Using TiO2 Nanoflower Clusters and Nanoparticles. *Mater. Lett.* 107, 210–213. doi:10.1016/j.matlet.2013.06.009

Jiang, Y., Li, M., Song, D., Li, X., and Yu, Y. (2014). A Novel 3D Structure Composed of Strings of Hierarchical TiO2 Spheres Formed on TiO2 Nanobelts with High Photocatalytic Properties. *J. Solid State. Chem.* 211, 90–94. doi:10.1016/j.jssc.2013.12.002

Kavan, L., Yum, J. H., and Grätzel, M. (2011). Graphene Nanoplatelets Outperforming Platinum as the Electrocatalyst in Co-bipyridine-mediated Dye-Sensitized Solar Cells. *Nano Lett.* 11, 5501–5506. doi:10.1021/nl203329c

Khalil, M., Anggraeni, E. S., Ivandini, T. A., and Budianto, E. (2019). Exposing TiO2 (001) crystal Facet in Nano Au-TiO2 Heterostructures for Enhanced Photodegradation of Methylene Blue. *Appl. Surf. Sci.* 487, 1376–1384. doi:10.1016/j.apsusc.2019.05.232

Konevskikh, T., Lukacs, R., and Kohler, A. (2018). An Improved Algorithm for Fast Resonant Mie Scatter Correction of Infrared Spectra of Cells and Tissues. *J. biophotonics* 11, e201600307. doi:10.1002/jbio.201600307

Lara, M. A., Jaramillo-Páez, C., Navío, J. A., Sánchez-Cid, P., and Hidalgo, M. C. (2019). Coupling of WO3 with Anatase TiO2 Sample with High {001} Facet Exposition: Effect on the Photocatalytic Properties. *Catal. Today* 328, 142–148. doi:10.1016/j.cattod.2018.11.012

Lee, C. S., Kim, J. K., Lim, J. Y., and Kim, J. H. (2014). One-Step Process for the Synthesis and Deposition of Anatase, Two-Dimensional, Disk-Shaped TiO2for Dye-Sensitized Solar Cells. *ACS Appl. Mater. Inter.* 6, 20842–20850. doi:10.1021/am505217k

Maurya, I. C., Singh, S., Senapati, S., Srivastava, P., and Bahadur, L. (2019). Green Synthesis of TiO2 Nanoparticles Using Bixa Orellana Seed Extract and its Application for Solar Cells. *Solar Energy* 194, 952–958. doi:10.1016/j.solener.2019.10.090

Oregan, B., and Grätzel, M. (1991). A Low-Cost, High-Efficiency Solar Cell Based on Dye-Sensitized Colloidal TiO2 films. *Nature* 353, 737–740. doi:10.1038/353737a0

Park, K.-H., and Dhayal, M. (2014). Simultaneous Growth of Rutile TiO2 as 1D/3D Nanorod/nanoflower on FTO in One-step Process Enhances Electrochemical Response of Photoanode in DSSC. *Electrochemistry Commun.* 49, 47–50. doi:10.1016/j.elecom.2014.09.011

Ponken, T., Kongsankham, S., Panya, S., Choawunklang, W., and Ardchongthong, P. (2019). Effect of Titanium Dioxide (TiO2) Light Scattering Layer Deposited by Spray Deposition Method at Room Temperature for Dye-Sensitized Solar Cell (DSSC). *Mater. Today Proc.* 17, 1249–1258. doi:10.1016/j.matpr.2019.06.013

Sauvage, F., Di Fonzo, F., Li Bassi, A., Casari, C. S., Russo, V., Divitini, G., et al. (2010). Hierarchical TiO2Photoanode for Dye-Sensitized Solar Cells. *Nano Lett.* 10, 2562–2567. doi:10.1021/nl101198b

Steffy, J. A. J., Kumar, P. N., Mary, J. S. S., Jeyarani, W. J., Tenkyong, T., Pugazhendhi, K., et al. (2017). Hierarchical Rutile TiO2 Heterostructures and Plasmon Impregnated TiO2/SnO2-Ag Bilayer Nanocomposites as Proficient Photoanode Systems. *Surf. Coat. Tech.* 310, 113–121.

Ünlü, B., and Özacar, M. (2020). Effect of Cu and Mn Amounts Doped to TiO2 on the Performance of DSSCs. *Solar Energy* 196, 448–456. doi:10.1016/j.solener.2019.12.043

Wang, G., Zhu, X., and Yu, J. (2015). Bilayer Hollow/spindle-like Anatase TiO2 Photoanode for High Efficiency Dye-Sensitized Solar Cells. *J. Power Sourc.* 278, 344–351. doi:10.1016/j.jpowsour.2014.12.091

Wang, Q., Moser, J.-E., and Grätzel, M. (2005). Electrochemical Impedance Spectroscopic Analysis of Dye-Sensitized Solar Cells. *J. Phys. Chem. B* 109 (31), 14945–14953. doi:10.1021/jp052768h

Wang, W., Liu, F., Wang, B., and Wang, Y. (2019). Effect of Defects in TiO2 Nanoplates with Exposed {001} Facets on the Gas Sensing Properties. *Chin. Chem. Lett.* 30, 1261–1265. doi:10.1016/j.cclet.2018.12.030

Wang, Y., Du, G., Liu, H., Liu, D., Qin, S., Wang, N., et al. (2008). Nanostructured Sheets of Ti]O Nanobelts for Gas Sensing and Antibacterial Applications. *Adv. Funct. Mater.* 18, 1131–1137. doi:10.1002/adfm.200701120

Xie, F., Dong, G., Wu, K., Li, Y., Wei, M., and Du, S. (2020). *In Situ* topological Transformation of Hierarchical TiO2 Hollow Nanobricks as Efficient Scattering Layer for Dye-Sensitized Solar Cells. *Chem. Phys. Lett.* 739, 136996. doi:10.1016/j.cplett.2019.136996

Xu, L., Xu, J., Hu, H., Cui, C., Ding, Z., Yan, Y., et al. (2019). Hierarchical Submicroflowers Assembled from Ultrathin Anatase TiO2 Nanosheets as Light Scattering Centers in TiO2 Photoanodes for Dye-Sensitized Solar Cells. *J. Alloys Comp.* 776, 1002–1008. doi:10.1016/j.jallcom.2018.10.386

Xue, G. G., Yu, X. R., Yu, T., Bao, C. X., Zhang, J. Y., Guan, J., et al. (2012). Understanding of the Chopping Frequency Effect on IPCE Measurements for Dye-Sensitized Solar Cells: from the Viewpoint of Electron Transport and Extinction Spectrum. *J. Phys. D: Appl. Phys.* 45, 425104. doi:10.1088/0022-3727/45/42/425104

Zhang, W., Chang, S. S., Gu, J. B., Yao, S. W., and Wang, H. Z. (2019). Metal-organic Frameworks Derived Porous Cake-like TiO2 as an Efficient Scattering Layer for Dye-Sensitized Solar Cells. *Int. J. Electrochem. Sci.* 14, 7166–7177. doi:10.20964/2019.08.62

Zhao, F., Ma, R., and Jiang, Y. (2018). Strong Efficiency Improvement in Dye-Sensitized Solar Cells by Novel Multi-Dimensional TiO2 Photoelectrode. *Appl. Surf. Sci.* 434, 11–15. doi:10.1016/j.apsusc.2017.10.131

Conflict of Interest: The authors declare that the research was conducted in the absence of any commercial or financial relationships that could be construed as a potential conflict of interest.